IJBPAS, November, 2024, 13(11): 5911-5928

ISSN: 2277–4998

International Journal of Biology, Pharmacy and Allied Sciences (IJBPAS)

'A Bridge Between Laboratory and Reader'

www.ijbpas.com

IN SILICO COMPUTATIONAL SCREENING OF PHYTOCONSTITUENTS OF POLYHERBAL FORMULATION SUKKUMALLI KASHAYAM AGAINST MPRO, SPIKE PROTEIN AND TMPRSS2 PROTEASE INHIBITOR FOR SARS-COV-2

PRIYA J*[1], ASHIKA BALKIS MN[2] AND LOGAPRIYA P[3]

1: Associate Professor, Department of Biochemistry, Ethiraj College for Women (Autonomous)

Chennai-600 008, Tamilnadu, India

2&3: PG Scholar, Department of Biochemistry, Ethiraj College for Women (Autonomous)

Chennai-600 008, Tamilnadu, India

***Corresponding Author: Dr. Priya.J: E Mail: priya_j@ethirajcollege.edu.in**

Received 24th Sept. 2023; Revised 25th Nov. 2023; Accepted 1st March. 2024; Available online 1st Nov. 2024

https://doi.org/10.31032/IJBPAS/2024/13.11.8481

ABSTRACT

The Outbreak of COVID-19 by SARS-CoV-2 infection caused severe acute respiratory syndrome has posed a serious threat to mankind across the world, with Wuhan as epicentre for its spread. These days, immunomodulators, antiviral medications, anti-SARS-CoV-2 monoclonal antibodies, anti-inflammatory medications, and vaccines are used to treat SARS-CoV-2. On the other hand, studies on the long-term risks associated with synthetic pharmaceuticals and COVID-19 vaccinations are currently in progress, which has allowed researchers to search for a different therapeutic agent that has less adverse effects. Since ancient times, both developed and developing nations have utilized herbal medicines to treat a variety of illnesses. Using *Insilico* computational evaluation, the current study aims to evaluate Sukkumalli Kashayam (SMK), a polyherbal formulation, for the existence of effective bioactive components against COVID-19. GC-MS analysis of SMK revealed the presence of 14 phytoconstituents, and the drug likeliness of 14 phytoconstituents was screened by web tool Swiss ADME. Of these, six components that complied with Lipinski's rule of five were chosen

for molecular docking studies against Mpro, Spikeprotein of SARS-CoV-2, and TMPRSS2 protease of host cell surface. Remdesivir, an antiviral drug, was employed as standard. The results showed that the phytoconstituents 4H-1-Benzopyran-4-one, 7-hydroxy-2-phenyl- demonstrated minimum binding energy of -7.34 Kcal/mol followed by Flavone (-7.32 Kcal/mol)against Mpro, while Coumarin-8-ol, 7-methoxy-4-methyl- utilizes the binding energy of -7.96 Kcal/mol against Spike protein then comes 4H-1-Benzopyran-4-one,7-hydroxy-2-phenyl-(-7.72Kcal/mol),flavone(-7.37Kcal/mol) and 2,3-dihydro-1-ethyl-1H-3-ethylcyclopenta[b]quinoxaline(-6.66 Kcal/mol),whereas 4H-1-Benzopyran-4-one, 7-hydroxy-2-phenyl- employs minimum binding energy of -7.61 Kcal/mol with TMPRSS2 protease followed by flavones(-7.08 Kcal/mol),Coumarin-8-ol,7-methoxy-4-methyl-(-6.5Kcal/mol),2,3-dihydro-1-ethyl-1H-3-methylcyclopenta[b]quinoxaline(-6.39 Kcal/mol). The study found that, in comparison to the conventional antiviral medication remdesivir, SMK possessed active main components that would be viable candidates against COVID-19.

Keywords: Sukkumalli kashayam, Mpro, Spikeprotein, TMPRSS2 protease, covid-19, In silico

INTRODUCTION

SARS-CoV-2/Corona Virus Disease 2019 (COVID-19) is an encased, constructive-sense, single-stranded RNA virus similar to severe acute respiratory syndrome (SARS) and Middle East Respiratory Syndrome (MERS) coronavirus **[1]**. This coronavirus was first identified in Wuhan, China, in December 2019 **[2]** and its outbreak has posed a severe burden to the global economic, medical, and public health infrastructure **[3]**. According to the World Health Organization (WHO)reports on COVID-19 on 21 October 2023, the prevalence of COVID-19 is about 771,679,618 people and 6,977,023 deaths globally. The COVID-19 is primarily a droplet-spread infection, and patients exhibit various symptoms of which fever, dry cough, and fatigue are predominant **[4]**. However older and comorbid people with diabetes, cardiovascular disease, chronic respiratory disease, and cancer developed severe symptoms like acute respiratory distress syndrome, metabolic acidosis, septic shock, coagulation dysfunction, eventually leading to multiple organ failure **[5-7]**, while mild or asymptomatic COVID-19 patients can recover shortly after isolation and healthy lifestyle and food habits **[8]**.

At present, different therapeutic managements are available under FDA-issued Emergency Use Authorization to control COVID-19 that includes remdesivir, bamlanivimab/etesevimab, casirivimab / imdevimab, dexamethasone, baricitinib, and tocilizumab. Also, several vaccines are approved to prevent COVID-19, such as

BNT162b2 vaccine, mRNA-1273 vaccine, Ad26.COV2. S vaccine and ChAdOx1 nCoV-19n **[9]**. The research on long term risk of covid-19 vaccines are underway and there may be a chance of the emergence of unknown serious or chronic side effects in the future. Since the conventional drugs do not prove to be much efficacious, exploring the traditional system of medicine could be a feasible and hopeful strategy **[10]**. India has an unmatched alternative system of medicine in the form of Ayurveda, Yoga, and Naturopathy, Unani, Siddha, Homeopathy, which is now jointly referred to as Ayush, recognized by the Government of India **[11-12]**. Siddha Medicine is one of India's oldest (5000 years old) and well-documented medical systems and is practiced mainly in South India, especially in Tamil Nadu and Sri Lanka, Malaysia, Singapore, and Mauritius, where Tamils live **[13]**. Siddha polyherbal formulations are potent against several causative agents such as influenza, chikungunya, dengue, tuberculosis, and have been used successfully by Siddha practitioners and ordinary citizens for the treatment of many diseases such as Kabasura Kudineer during influenza outbreaks, Nilavembu Kashayam for dengue fever and several polyherbal formulations that have long been used for different health problems **[14-18]**. One such polyherbal formulation is Sukkumalli Kashayam, which is primarily made of Zingiber officinale (dry ginger also known as Sukku in Tamil) and Coriandrum sativum (coriander seeds also known as Malli in Tamil), these components are blended with three other ingredients, including Cuminum cyminum (cumin), Pepper nigrum (black pepper), Syzygium aromaticum (clove) and are evaluated against SARS-CoV-2 targets through *Insilico* techniques. In most of part of South India, Sukkumalli kashayam is consumed as tea or coffee to strengthen immunity, relieve the common cold or flu, and help with indigestion. Although it has several health benefits and can be used to cure a wide range of illnesses, there is no scientific evidence to support its claims. This work aims to demonstrate the potential therapeutic agent of these polyherbal formulations against SARS-CoV-2.

MATERIALS AND METHODS

PLACE OF WORK

The research work was carried out in the PG department of Biochemistry, Ethiraj College for Women, Chennai.

COLLECTION OF SAMPLES

Ginger, Coriander seeds, Cumin, Black Pepper and Clove were purchased from an organic store at Pammal, Chennai District, Tamil Nadu. Dry samples of Ginger, Coriander seeds, Cumin, Black Pepper and Clove of ratio 10:10:5:5:1 were grinded, and the coarse powder obtained was stored in a sterile airtight container for further study.

PREPARATION OF EXTRACT

The extract was prepared by decoction process by dissolving 25 gm of powder in 400ml of distilled water and heated at 50-60ºC till the mixture gets reduced to half the of the volume (200 ml). After cooling the mixture, it was filtered using a muslin cloth and the filtrate was concentrated in an incubator at 45ºC. The crude extract obtained was stored in a sterile container at 2-5ºC until the completion of study and the resulting Sukkumalli kashayam extract was designated as SMK. The yield of SMK was calculated as follows:

% Yield= (Weight of the extract /Weight of the sample) ×100

GAS CHROMATOGRAPHY–MASS SPECTROMETRY (GC-MS)

The GC-MS analysis of the aqueous extract ofSMK was carried out and the extract was injected into a HP-5 column (30 m X 0.25 mm i.d with 0.25 µm film thickness), Agilent technologies 6890 N JEOL GC Mate II GC-MS model. Following chromatographic conditions were used: Helium as carrier gas, flow rate of 1 mL/min; and the injector was operated at 200ºC and column oven temperature was programmed as 50-250ºC at a rate of 10ºC/min injection mode and following MS conditions were used: ionization voltage of 70 eV, ion source temperature of 250ºC, interface temperature of 250ºC; mass range of 50-600 mass units **[19]**. The database of the National Institute Standard and Technology (NIST) having more than 62,000 patterns was used for the interpretation of the mass spectrum of GC-MS. Tmass spectrum of the unknown component was compared with the spectrum of the known components stored in the NIST library.

PROTEIN PREPARATION

The x-ray diffraction structure of Mpro (PDB ID: 7SET), Spike protein (PDB ID: 7B62), and TMPRSS2 protease (PDB ID: 7MEQ) are retrieved from the Research Collaboratory for Structural Bioinformatics (RCSB) Protein Data Bank, to which the heteroatoms are removed manually for the effective binding of ligand to the protein.

LIGAND PREPARATION

The details of the bioactive compounds present in SMK such as IUPAC name, canonical smiles, molecular formula, and weight were retrieved from the PubChem database. The 2D structure of the compounds are generated through smiles by using ACD/chemsketch, is then converted to 3D structure **(Figures 1, 2, 3)** followed by 3D optimization and saved as MDL-MOL file format and converted into PDB format using open babel software **[20]**.

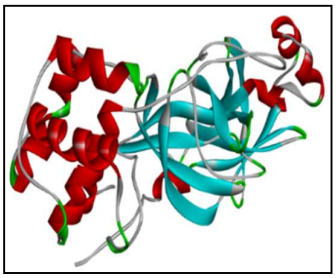

Figure 1: Main protease

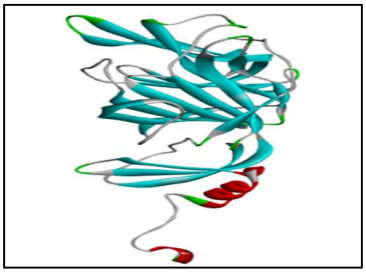

Figure 2: Spike

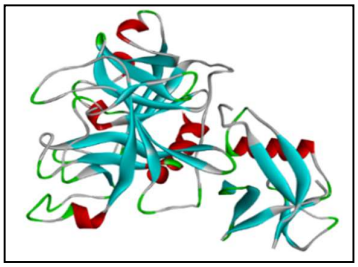

Figure 3: TMPRSS2

ACTIVE SITE PREPARATION

Active sites for Mpro and Spike protein were predicted by using PDB SUM, and the active sites for TMPRSS2 protein were predicted by using the CastP server.

SWISS ADME AND TOXICITY ANALYSIS

Drug-like properties were calculated using Lipinski's rule of five, using a free web tool Swiss ADME. Among the 14 phytoconstituents identified by GC-MS, 6 compounds that adhere with Lipinski rule of 5 were selected for docking, while 8 compounds violated the rule were eliminated. This helps to reduce the risks and intensify the success in the drug development process.

MOLECULAR DOCKING

Molecular docking studies were performed for the selected compounds using Autodock 4.2.6 software tool for identifying the binding energy between each ligand and the target proteins namely, Mpro, Spike protein, and TMPRSS2. To the 3D structure of target proteins hydrogen molecules and Kollman charges are added. In ligand preparation centre node and rotatable bonds were selected and saved in pdbqt format. In grid preparation, the active sites of the target proteins are selected by adjusting the grids. For the Mpro, spacing of 0.375 and the dimensions of x, y, z was set to 60 × 76 × 66; For Spike protein, spacing of 0.375 and the dimensions of x, y, z was set to 96 × 84 × 76; while for TMPRSS2, spacing of 0.375 and the dimensions of x, y, z was set to 54 × 40 × 62 was set and saved in GPF format and subjected to run. In the docking procedure, the Lamarckian genetic algorithm was selected for flexible ligand-receptor docking **[21]**.

DOCKING VISUALIZATION

The bonded and non-bonded interactions between the ligand and the target proteins were visualized using Biovia Discovery Studio Visualizer. This tool is utilized to depict various interactions such as hydrogen bond, hydrophobic and Vanderwal's interactions.

RESULTS& DISCUSSION

PERCENTAGE YIELD OF EXTRACT

Decoction process involves continuous hot extraction using specified volume of water as a solvent for a definite time; which is then cooled, filtered and processed for further use. The extraction of SMK obtained by decoction process was weighed, and the extraction yield obtained was found to be 58.98±2.3005%.

IDENTIFICATION OF BIOACTIVE COMPOUNDS

The compounds identified from GC-MS analysis was represented in the **Table 1** and the chromatogram presented in **Figure 4**. The compound, 4H-1-Benzopyran-4-one, 7-hydroxy-2-phenyl- has attained a highest peak area of 39.17% followed by the compounds Heptadecanoic acid, 16-methyl, methyl ester (31.09%), Coumarin-8-ol, 7-methoxy-4-methyl- (8.48%), Hexadecenoic acid, methyl ester (7.22%), 1-Docosene (4.02%), 4-hydroxy-3-methoxybenzyl alcohol(2.64%), Oleicacid(1.55%), 2,3-dihydro-1-ethyl-1H-3-methylcyclopenta[b]quinoxaline (1.31%), 1-Tetracosanol (1.24%), 1-Hexacosene (1.09%), flavone (0.73%), Thujopsene-**[12]** (0.72%), 1-Eicosene (0.68%), and Nonanoic acid, 1-methylethyl ester (0.02%).

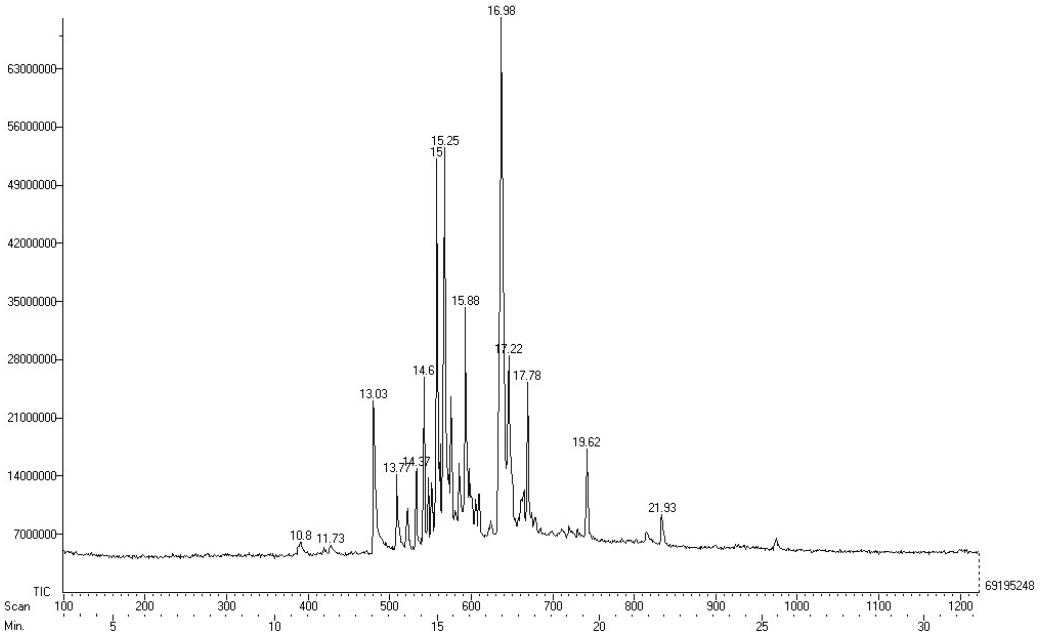

Figure 4: GC-MS spectra of aqueous extract of SMK

Table 1: GC-MS analysis of SMK

Peak name	Chemical Formula	Mol Wt	Retention time (mins)	Peak Area (mm)	% Peak Area
Coumarin-8-ol, 7-methoxy-4-methyl-	$C_{11}H_{10}O_4$	206.0	13.77	32034680	8.48%
Oleic acid	$C_{18}H_{34}O_2$	282.0	16.98	5891368	1.55%
Heptadecanoic acid, 16-methyl-, methyl ester	$C_{19}H_{38}O_2$	298.0	17.22	117474536	31.09%
2,3-dihydro-1-ethyl-1H-3-methylcyclopenta[b]quinoxaline	$C_{14}H_{16}N_2$	212.0	14.37	4958824	1.31%
1-Hexacosene	$C_{26}H_{52}$	364.0	21.93	4104280	1.09%
hydroxy-3-methoxybenzyl alcohol	$C_8H_{10}O_3$	154.0	10.8	9979716	2.64%

4H-1-Benzopyran-4-one, 7-hydroxy-2-phenyl-	$C_{15}H_{10}O_3$	238.0	15	148024000	39.17%
Flavone	$C_{15}H_{10}O_2$	222.0	14.6	2773672	0.73%
Nonanoic acid, 1-methylethyl ester	$C_{12}H_{24}O_2$	200.0	11.73	95320	0.02%
1-Docosene	$C_{22}H_{44}$	308.0	17.78	15208568	4.02%
Tetracosanol	$C_{24}H_{50}O$	354.0	19.62	4696056	1.24%
Thujopsene-[12]	$C_{15}H_{24}$	204.0	13.03	2729452	0.72%
Hexadecenoic acid, methyl ester	$C_{17}H_{34}O_2$	270.0	15.25	27294520	7.22%
1-Eicosene	$C_{20}H_{40}$	280.0	15.88	2582336	0.68%

SWISS ADME AND TOXICITY ANALYSIS

The absorption, distribution, metabolism, and excretion (ADME) of substances play an essential role in the drug development phase and were predicted by a free web tool SwissADME. It is very important for a drug to satisfy the Lipinski rule of five in order to be administered orally **[22]** and it also used to evaluate the durability of a compound. As per Lipinski's rule, molecular weight should be less than 500 DA; Hydrogen Bond donor should be less than or equivalent to 5; hydrogen bond acceptor should be less than or equivalent to 10. Molecular weight is related to molecular size, as molecular size increases solubility decreases and results in poor absorption as it affects the passage through biological membrane **[23]**. The Increase in hydrogen bond donor and acceptor affect the membrane partition and permeability of the drug that results in decrease affinity towards hydrophobic site **[24]**. LogP of a compound should be 5, increase in logP decreases aqueous solubility, and result in poor absorption **[25]** more than 10 rotatable bonds have deleterious effect on permeation rate **[26]**. The selected phytoconstituents that adhere to Lipinski's rules of five is shown in **Table 2**, and their ADME findings confirm that SMK possess phytoconstituents that are orally active drugs compared to that of standard remdesivir which has been reported to have higher molecular weight, increased H acceptor and violation of rule.

Table 2: Absorption, Distribution, Metabolism, and Excretion (ADME) parameters

Compound	Mol Wt	H Donor	H Acceptor	Log P	Log S	GI Absorption	BBB Permeant	P-Gp substrate	Violation
Coumarin-8-ol, 7-methoxy-4-methyl-	206.0	1	4	1.44	-2.45	High	Yes	No	0
2,3-dihydro-1-ethyl-1H-3-methylcyclopenta[b]quinoxaline	212.0	0	2	2.95	-3.41	High	Yes	Yes	0
4-hydroxy-3-methoxybenzyl alcohol	154.0	2	3	-0.02	-1.05	High	Yes	No	0
4H-1-Benzopyran-4-one, 7-hydroxy-2-phenyl	238.0	1	3	3.62	-4.19	High	Yes	No	0
Flavone	222.0	0	2	3.56	-4.09	High	Yes	No	0
Nonanoicacid, 1-methylethyl ester	200.0	0	2	5.12	-3.71	High	Yes	No	0
Remdesivir (Std)	602.6	4	12	1.91	-4.12	Low	No	Yes	2

MOLECULAR DOCKING

Molecular docking is used to locate the ligands into the target receptor in an optimized orientation and it predicts the binding affinity and energy of the ligands docked to the binding sites of the target receptor. The objective of the molecular docking is finding a best orientation between the ligand and the receptor that resulting in a minimum energy required in binding to the target of interest **[27]**. Molecular docking of ligands to the target protein will interpret interactions and help in the development of novel drugs against the inhibition of potential drug target in the field of drug discovery and development. The inhibition of target protein is determined by knowing the binding affinity and based on the bond formation of the most potent molecule. Lower the binding energy of a compound docked to target, greater is the binding efficiency. Greater the hydrogen bonds interaction between the ligand and the target determines the strength of binding **[28]**. In the present study, docking was performed for 6 phytoconstituents present in SMK namely, Coumarin-8-ol 7-methoxy-4-methyl-, 4-hydroxy-3-methoxybenzyl alcohol, 2,3-dihydro-1-ethyl-1H-3-methylcyclopenta[b]quinoxaline, 4H-1-Benzopyran-4-one 7-hydroxy-2-phenyl-, flavone, Nonanoic acid 1-methylethyl ester against Mpro, Spike of SARS-COV-2 and TMPRSS2 by utilizing Autodock tool V 1.5.6. The best conformations were chosen based on the least binding energy. The bonded and non-bonded interactions such as hydrogen bond, van der waals are visualized using Biovia Discovery Studio Visualizer software.

Table 3: Inhibition constant, energy values of docking simulation of SMK compounds with targets Mpro, Spike protein and TMPRSS2

SMK compounds	Inhibition constant (μM)	Binding energy	Ligand efficiency	Intermolecular energy	vdW + Hbond + desolv energy	Electro-static energy	Torsional energy	Total internal unbound	ref RMS
Mpro with SMK compounds									
Coumarin-8-ol, 7-methoxy-4-methyl-	13.69	-6.64	-0.44	-7.23	-7.01	-0.22	0.6	-0.58	32.56
2,3-dihydro-1-ethyl-1H-3-methylcyclopenta[b]quinoxaline	22.32	-6.35	-0.4	-6.64	-6.62	-0.03	0.3	-0.1	33.38
4-hydroxy-3-methoxybenzyl alcohol	321.38	-4.77	-0.43	-5.96	-5.71	-0.25	1.19	-0.53	33.82
4H-1-Benzopyran-4-one, 7-hydroxy-2-phenyl-	4.19	-7.34	-0.41	-7.93	-7.89	-0.05	0.6	-0.29	41.95
Flavone	4.32	-7.32	-0.43	-7.62	-7.61	0.0	0.3	-0.32	36.95
Nonanoic acid, 1-methylethyl ester	523.65	-4.48	-0.32	-7.16	-7.07	-0.09	2.68	-0.46	37.6
Remdesivir (Std)	4.47	-7.3	-0.17	-12.37	-12.1	-0.27	5.07	-4.53	35.86
Spike protein with SMK compounds									
Coumarin-8-ol, 7-methoxy-4-methyl-	1.45	-7.96	-0.53	-8.56	-8.17	-0.4	0.6	-0.32	51.41
2,3-dihydro-1-ethyl-1H-3-	13.14	-6.66	-0.42	-6.96	-6.96	0.01	0.3	-0.1	50.45

methylcyclopenta[b]quinoxaline									
4-hydroxy-3-methoxybenzyl alcohol	**208.31**	**-5.02**	**-0.46**	**-6.22**	**-6.07**	**-0.15**	**1.19**	**-0.53**	**51.09**
4H-1-Benzopyran-4-one, 7-hydroxy-2-phenyl-	**2.21**	**-7.72**	**-0.43**	**-8.31**	**-8.31**	**-0.01**	**0.6**	**0.28**	**50.4**
Flavone	**3.95**	**-7.37**	**-0.43**	**-7.67**	**-7.72**	**0.05**	**0.3**	**-0.32**	**55.22**
Nonanoic acid, 1-methylethyl ester	**81.23**	**-5.58**	**-0.4**	**-8.26**	**-8.15**	**-0.11**	**2.68**	**-0.8**	**48.18**
Remdesivir (Std)	**13.64**	**-6.64**	**-0.16**	**-11.71**	**-10.92**	**-0.79**	**5.07**	**-5.16**	**30.55**
TMPRSS2 with SMK compounds									
Coumarin-8-ol, 7-methoxy-4-methyl-	**17.27**	**-6.5**	**-0.43**	**-7.09**	**-6.99**	**-0.1**	**0.6**	**-0.6**	**31.96**
2,3-dihydro-1-ethyl-1H-3-methylcyclopenta[b]quinoxaline	**20.7**	**-6.39**	**-0.4**	**-6.69**	**-6.64**	**-0.05**	**0.3**	**-0.12**	**34.26**
4-hydroxy-3-methoxybenzyl alcohol	**58.77**	**-5.77**	**-0.52**	**-6.97**	**-6.79**	**-0.18**	**1.19**	**-0.17**	**33.86**
4H-1-Benzopyran-4-one, 7-hydroxy-2-phenyl-	**2.62**	**-7.61**	**-0.42**	**-8.21**	**-8.05**	**-0.16**	**0.6**	**-0.29**	**34.16**
Flavone	**6.5**	**-7.08**	**-0.42**	**-7.38**	**-7.37**	**-0.01**	**0.3**	**-0.32**	**30.26**
Nonanoic acid, 1-methylethyl ester	**142.26**	**-5.25**	**-0.38**	**-7.93**	**-7.88**	**-0.05**	**2.68**	**-0.92**	**33.18**
Remdesivir (Std)	**35.0**	**-6.08**	**-0.14**	**-11.15**	**-11.07**	**-0.08**	**5.07**	**-4.62**	**30.64**

Table 4: Molecular docking result analysis of bioactive compounds from SMK against Mpro, spike protein, TMPRSS2

Compound name		Binding Energy Kcal/mol	No of Vander Waal's interaction	No. of hydrogen bonds	Hydrogen bond interaction	Interacted residues with ligand
Coumarin-8-ol, 7-methoxy-4-methyl-	**Mpro**	**-6.64**	**Met165, Glu166, His163, Phe140, Asn142, Thr26**	**4**	**Cys145, Gly143, Leu141, Ser144**	**Met165, Glu166, His163, Phe140, Asn142, Thr26, Cys145, Gly143, Leu141, Ser144, His172, Leu27**
	Spike Protein	**-7.96**	**Glu54, Asn450, Thr345**	**3**	**Asp442, Arg58, Asn448**	**Glu54, Asn450, Thr345, Asp442, Arg58, Asn448, Tyr451, Asp56, Arg509, Leu441, Trp33, Arg346, Trp100**
	TMPRSS2	**-6.5**	**Phe311, Phe321, His274, Asn277, His307**	**3**	**Gly323, Thr309, Gln276**	**Phe311, Phe321, His274, Asn277, His307, Gly323, Thr309, Gln276, Tyr322, Val275**
2,3-dihydro-1-ethyl-1H-3-methylcyclopenta[b]quinoxaline	**Mpro**	**-6.35**	**Thr25, His41, His164, Thr26, Phe140, Ser144, Leu141, Asn142**	**1**	**Gly143**	**Thr25, His41, His164, Thr26, Phe140, Ser144, Leu141, Asn142, Gly143, Cys145, His163, Leu27**
	Spike Protein	**-6.66**	**Glu54, Asn450, Asp56, Arg58, Leu441, Arg509, Asp442, Phe347, Ser349**	**0**	**-**	**Glu54, Asn450, Asp56, Arg58, Leu441, Arg509, Asp442, Phe347, Ser349, Trp33, Arg346, Tyr52, Tyr451**
	TMPRSS2	**-6.39**	**Phe321, Phe311, Gln327, Trp306, His307, His274, Asn277**	**1**	**Gly323**	**Phe321, Phe311, Gln327, Trp306, His307, His274, Asn277, Gly323, Tyr322, Thr309**
4-hydroxy-3-methoxybenzyl alcohol	**Mpro**	**-4.77**	**Met165, His172, His163, Ser144, Leu141**	**4**	**Phe140, Glu166, Asn142, Gly143**	**Met165, His172, His163, Ser144, Leu141, Phe140, Glu166, Asn142, Gly143, Cys145**
	Spike Protein	**-5.02**	**Asn450, Asp442, Leu441, Glu54**	**4**	**Asp56, Tyr451, Phe347, Thr345**	**Asn450, Asp442, Leu441, Glu54, Asp56, Tyr451, Phe347, Thr345, Tyr52, Trp33, Arg346, Arg509**

	TMPRSS2	**-5.77**	**Gln276, Val275, His307, Asn277, Tyr322, Phe311, Ala324, His274**	**4**	**Gly323, Gly325, Phe321, Thr309**	**Gln276, Val275, His307, Asn277, Tyr322, Phe311, Ala324, His274, Gly323, Gly325, Phe321, Thr309**
4H-1-Benzopyran-4-one, 7-hydroxy-2-phenyl-	**Mpro**	**-7.34**	**Ala191, Gln192, Gln189, Arg188, Tyr54**	**2**	**Glu166, Thr190**	**Ala191, Gln192, Gln189, Arg188, Tyr54, Glu166, Thr190, His41, Met49, Met165, Asp187**
	Spike Protein	**-7.72**	**Asp56, Glu54, Asn450, Thr345, Leu441, Asp442, Arg58, Phe347, Ala348**	**1**	**Ser349**	**Asp56, Glu54, Asn450, Thr345, Leu441, Asp442, Arg58, Phe347, Ala348, Ser349, Arg509, Trp33, Arg346, Tyr451**
	TMPRSS2	**-7.61**	**Val275, Gln276, His307, Trp306, Gln327, Gly325, Ala324, Phe311, His274**	**3**	**Asn277, Gly323, Phe321**	**Val275, Gln276, His307, Trp306, Gln327, Gly325, Ala324, Phe311, His274, Asn277, Gly323, Phe321, Tyr322, Thr309,**
Flavone	**Mpro**	**-7.32**	**Tyr54, Arg188, Gln189, Thr190**	**1**	**Glu166**	**Tyr54, Arg188, Gln189, Thr190, Glu166, Met165, Met49, His41, Asp187**
	Spike Protein	**-7.37**	**Glu54, Asp56, Arg58, Trp33, Leu441, Thr345, Arg509, Phe347, Ala348**	**2**	**Asp450, Asn448**	**Glu54, Asp56, Arg58, Trp33, Leu441, Thr345, Arg509, Phe347, Ala348, Asn450, Asn448, Arg346, Asp442, Tyr451, Ser349**
	TMPRSS2	**-7.08**	**Gln276, His307, Trp306, Gln327, Phe321, Gly323, Phe311, His274, Val275**	**1**	**Asn277**	**Gln276, His307, Trp306, Gln327, Phe321, Gly323, Phe311, His274, Val275, Asn277, Thr309, Tyr322**
Nonanoic acid, 1-methylethyl ester	**Mpro**	**-4.48**	**Phe140, Leu141, Ser144, Asp187, Tyr54, His164, Met165**	**1**	**Gly143**	**Phe140, Leu141, Ser144, Asp187, Tyr54, His164, Met165, Gly143, Asn142, His163, Cys145, His41, Met49**
	Spike Protein	**-5.58**	**Leu441, Thr345, Arg509, Asn450, Asp442, Asp56, Phe347**	**2**	**Asn448, Arg58**	**Leu441, Thr345, Arg509, Asn450, Asp442, Asp56, Phe347, Asn448, Arg58, Arg346, Trp33, Val98, Tyr451, Trp100,**
	TMPRSS2	**-5.25**	**Thr309, Gln327, His307, Trp306, Gln276, Asn277, His274, Phe311, Phe321**	**3**	**Gly323, Ala324, Gly325**	**Thr309, Gln327, His307, Trp306, Gln276, Asn277, His274, Phe311, Phe321, Gly323, Ala324, Gly325, Tyr322**
Remdesivir (Std)	**Mpro**	**-7.3**	**Gly143, Leu141, His163, Phe140, Asp187, Leu167, Thr190, Ala191, Gln192, Gln189,**	**4**	**Ser144, Asn142, Cys145, Glu166**	**Gly143, Leu141, His163, Phe140, Asp187, Leu167, Thr190, Ala191, Gln192, Gln189, Ser144, Asn142, Cys145, Glu166, His164, Arg188, His41, Met165, Met49**
	Spike Protein	**-6.64**	**Tyr49, Tyr100, Gln414, Ile410, Gln409, Asp100, Gly404**	**7**	**Asp50, Tyr99, Arg408, Lys378, Asn53, Ser53, Val407**	**Tyr49, Tyr100, Gln414, Ile410, Gln409, Asp100, Gly404, Asp50, Tyr99, Arg408, Lys378, Asn53, Ser53, Val407, Thr376, Phe377, Ala411, Tyr508**
	TMPRSS2	**-6.08**	**Gln327, His307, Trp308, Gly323, Ala324, Phe311, Val275, His274, Asn277**	**2**	**Trp306, Phe321**	**Gln327, His307, Trp308, Gly323, Ala324, Phe311, Val275, His274, Asn277, Trp306, Phe321, Thr309, Gln276, Gly325, Tyr322**

Mpro is main protease, a proteolytic key enzyme which supports the life cycle of the virus by cleaving the polyproteins translated from RNA which give rise to functional viral proteins **[29]**. Inhibition of main protease results in reduced assembly of functional viral proteins as their proteolytic action is inhibited **[30]**. From docking analysis of Mpro **(Table 3)**, the compound 4H-1-Benzopyran-4-one, 7-hydroxy-2-phenyl- utilizes the minimum binding energy of -7.34 Kcal/mol with Mpro followed by the compound Flavone(-7.32 Kcal/mol), Coumarin-8-ol, 7-methoxy-4-methyl- (-6.64 Kcal/mol), 2,3-dihydro-1-ethyl-1H-3-methylcyclopenta[b]quinoxaline (-6.35 Kcal/mol). The compound 4H-1-Benzopyran-4-one, 7-hydroxy-2-phenyl- forms two hydrogen bond interactions with amino acid GLU166, THR190 residues, flavone forms one hydrogen bond interaction with amino acid GLU166 residue, Coumarin-8-ol, 7-methoxy-4-methyl- forms four hydrogen bond interaction Cys145, Gly143, Leu141, Ser144. and 2,3-dihydro-1-ethyl-1H-3-methylcyclopenta[b]quinoxaline forms one hydrogen bond interaction with Gly143 **(Table 4, Figure 5)**. Amino acids GLY143 and GLU166 were found to be key residues that form hydrogen bonds with majority of the compounds. The standard remdesivir reported minimum binding energy of -7.3 Kcal/mol similar to that of 4H-1-Benzopyran-4-one, 7-hydroxy-2-phenyl- and flavone. The study revealed that the phytoconstituents of SMK possess potential binding affinity to inhibit Mpro and act as anti-SARS-CoV-2 compared to standard remdesivir.

Spike glycoprotein present on the surface of the virus mediates in the recognition of angiotensin converting enzyme-2 receptors, and also helps in the cell membrane fusion process **[31]**. Disrupting the interaction of spike protein and ACE-2 receptor is necessary to prevent the host cell to be infected. Therefore, Inhibition of spike protein prevents the virus to gain entry into the cell **[32]**. Docking analysis of Spike protein(Table:3), the compound Coumarin-8-ol, 7-methoxy-4-methyl- utilizes the binding energy of -7.96 Kcal/mol with Spike protein followed by the compound 4H-1-Benzopyran-4-one, 7-hydroxy-2-phenyl-(-7.72 Kcal/mol) flavone (-7.37 Kcal/mol), 2,3-dihydro-1-ethyl-1H-3-methylcyclopenta[b]quinoxaline (-6.66 Kcal/mol). The compound Coumarin-8-ol, 7-methoxy-4-methyl- forms three hydrogen bond interaction with amino acid ASN448, ARG58, ASP442 residues, while 4H-1-Benzopyran-4-one, 7-hydroxy-2-phenyl- formed one hydrogen bond interaction with amino acid SER349 residue and flavone two hydrogen bond interaction with amino acids Asp450, Asn448.Babcock and co-workers **[33]** reported that the amino acids positioned

at the 270-510 are essential for the SARS-CoV-2 virus to attach with the host cell ACE2 receptor. The results of the study revealed that Coumarin-8-ol, 7-methoxy-4-methyl- and 4H-1-Benzopyran-4-one and flavone were found ligand binding with the amino acids positioned at the 270-510 **(Table 4, Figure 6)** which limit the invasion of virus and thereby act as a possible inhibitors of Spike protein compared to the standard remdesivir (-6.64 Kcal/mol)

TMPRSS2 is a host cell surface protease that is highly susceptible to SARS-CoV-2 infection and plays a key role in the activation of spike glycoprotein by cleaving it. The priming activity of TMPRSS2 allows the virus to gain entry into the host cell **[34]**. TMPRSS2 inhibition results in incomplete cleavage of spike protein thereby hinder the virus entry into the host cell **[35]**. TMPRSS2 is among the most promising non-viral therapeutic targets to act as novel anti-COVID-19. Docking analysis of TMPRSS2 protease **(Table 3)** showed that the phytoconstituents 4H-1-Benzopyran-4-one, 7-hydroxy-2-phenyl- utilizes the minimum binding energy of -7.61 Kcal/mol with TMPRSS2 protease followed by flavones (-7.08 Kcal/mol), Coumarin-8-ol,7-methoxy-4-methyl-(-6.5Kcal/mol),2,3-dihydro-1-ethyl-1H-3-methylcyclopenta[b] quinoxaline (-6.39 Kcal/mol) and standard remdesivir (-6.08 Kcal/mol). The compound 4H-1-Benzopyran-4-one, 7-hydroxy-2 phenyl- formed three hydrogen bond interactions with amino acid ASN277, PHE321, GLY323 residues, flavone formed one hydrogen bond interaction with amino acid ASN277 residue, Coumarin-8-ol, 7-methoxy-4-methyl- formed three hydrogen bond interaction with Gly323, Thr309, Gln276 and 2,3-dihydro-1-ethyl-1H-3-methylcyclopenta[b]quinoxaline formed one hydrogen bond interaction with Gly323 **(Table 4, Figure 7)**. The docking interactions of 4H-1-Benzopyran-4-one, 7-hydroxy-2-phenyl-, flavones and Coumarin-8-ol, 7-methoxy-4-methyl- support docking results and the potential of these compounds to act as anti-COVID agent.

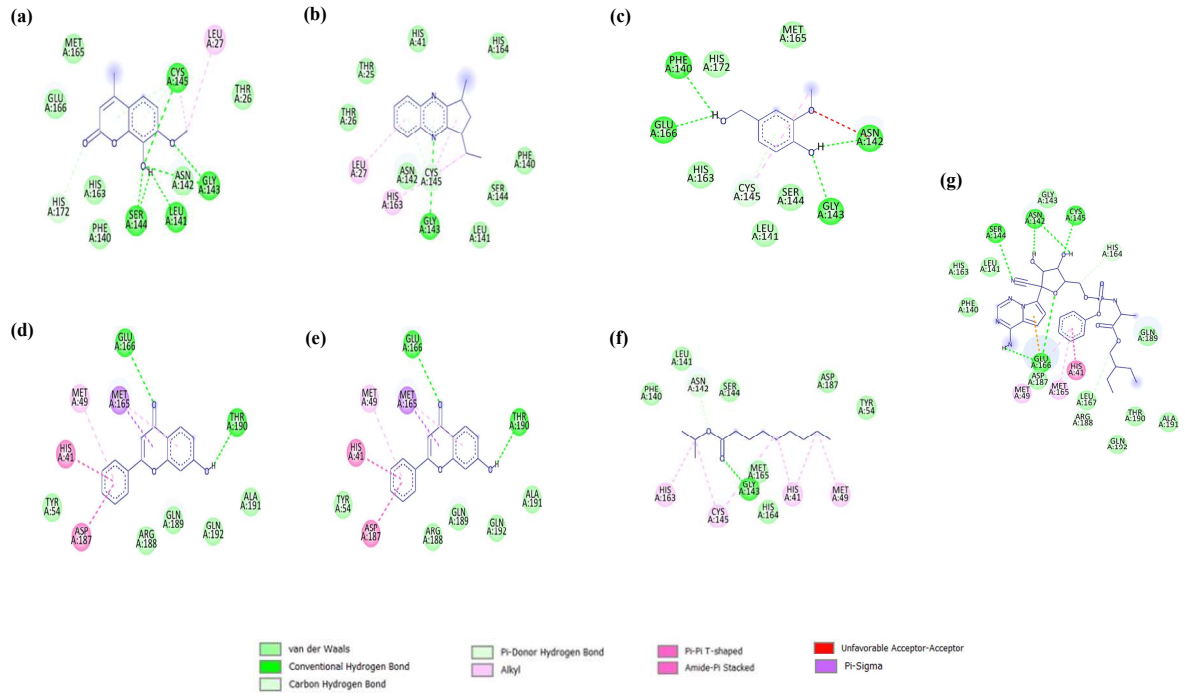

Figure 5: 2D structure of Mpro binding with a) Coumarin-8-ol, 7-methoxy-4-methyl-b) 2,3-dihydro-1-ethyl-1H-3-methylcyclopenta[b]quinoxaline c) 4-hydroxy-3-methoxybenzyl alcohol d) 4H-1-Benzopyran-4-one, 7-hydroxy-2-phenyl e) Flavone f) Nonanoic acid, 1-methylethyl ester g) Remdesivir

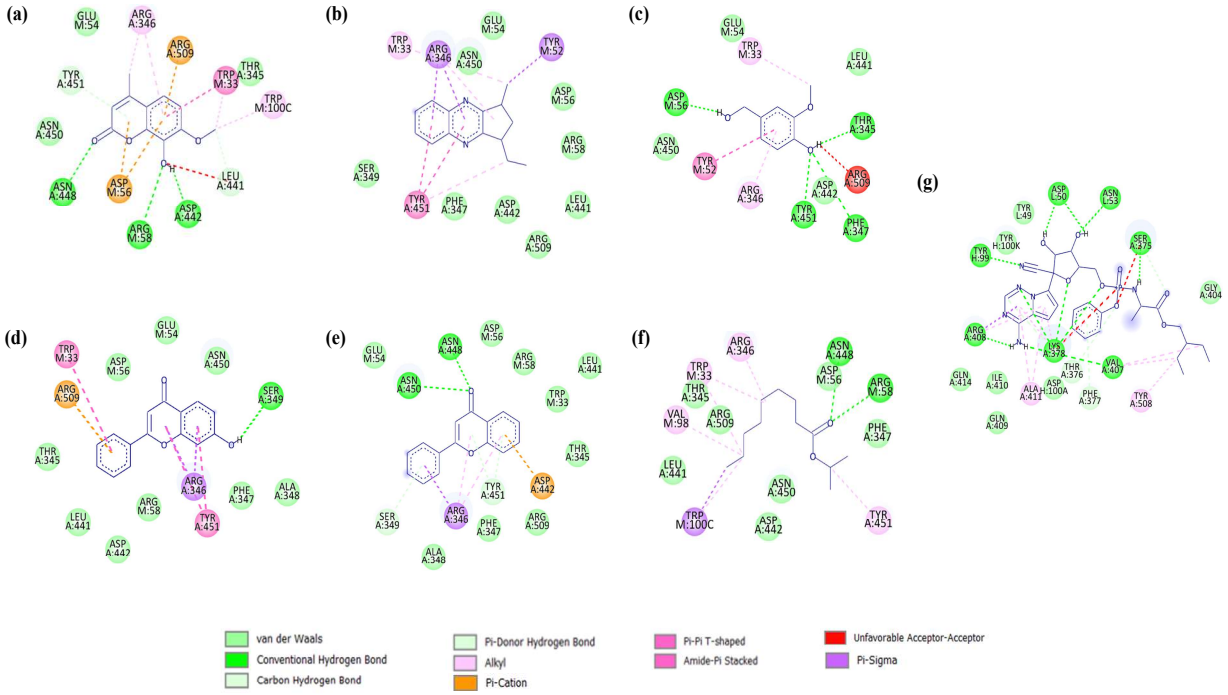

Figure 6 :2D structure of Spike protein binding with a) Coumarin-8-ol, 7-methoxy-4-methyl-b) 2,3-dihydro-1-ethyl-1H-3-methylcyclopenta[b]quinoxaline c) 4-hydroxy-3-methoxybenzyl alcohol d) 4H-1-Benzopyran-4-one, 7-hydroxy-2-phenyl e) Flavone f) Nonanoic acid, 1-methylethyl ester g) Remdesivir

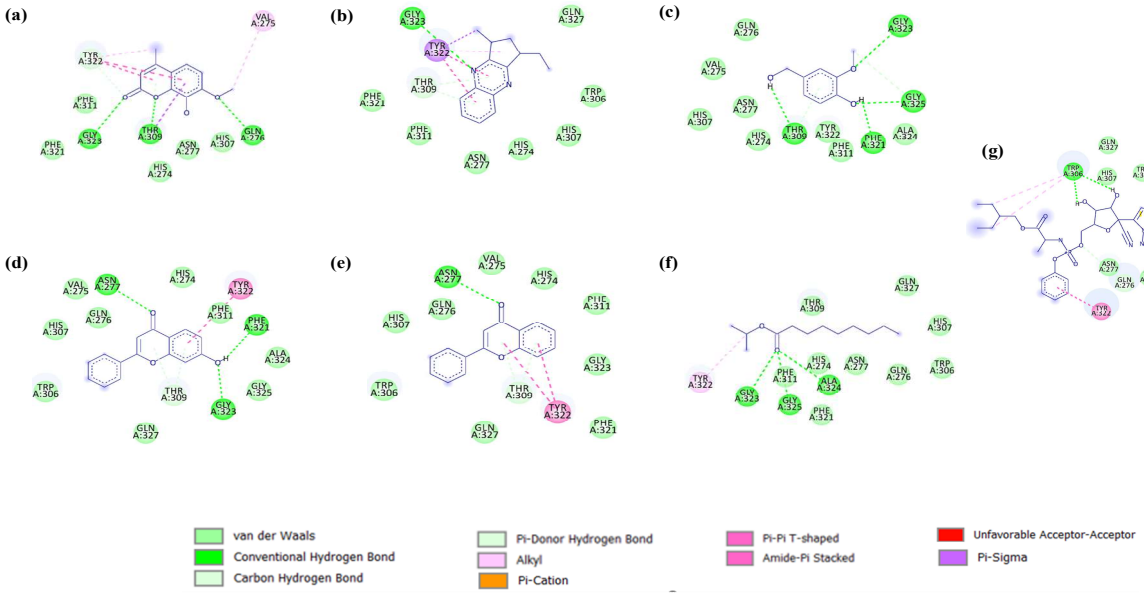

Figure 7 :2D structure of TMPRSS2 Proteasebinding with a) Coumarin-8-ol, 7-methoxy-4-methyl-b) 2,3-dihydro-1-ethyl-1H-3-methylcyclopenta[b]quinoxaline c) 4-hydroxy-3-methoxybenzyl alcohol d) 4H-1-Benzopyran-4-one, 7-hydroxy-2-phenyl e) Flavone f) Nonanoic acid, 1-methylethyl ester g) Remdesivir

CONCLUSION

Molecular docking has become a promising tool for drug development that limited the time and effort in drug designing.The computation screening of the current study revealed the presence of potential drug candidates in SMK that exhibited strong binding affinity against Mpro, Spike protein of SARS-CoV-2 and also displayed inhibition of TMPRSS2 protease there by blocking the infection in host.Therefore, including this SMK in the diet might not only act as anti-viral agent but also as non-viral therapeutic agent that prevent the occurrence of COVID -19, however more in vivo experimental research is required to validate the present study and develop potent drug against SARS-CoV-2.

REFERENCES

[1] Zhang T, Wu Q, Zhang Z. Probable pangolin origin of SARS-CoV-2 associated with the COVID-19 outbreak. Current biology. 2020;30(7):1346-51.

[2] Kaye AD, Okeagu CN, Pham AD, Silva RA, Hurley JJ, Arron BL, Sarfraz N, Lee HN, Ghali GE, Gamble JW, Liu H. Economic impact of COVID-19 pandemic on healthcare facilities and systems: International perspectives. Best Practice & Research Clinical Anaesthesiology. 2021;35(3):293-306.

[3] Andersen KG, Rambaut A, Lipkin WI, Holmes EC, Garry RF. The

proximal origin of SARS-CoV-2. Nature medicine. 2020;26(4):450-2.

[4] Chen B, Liu M, Huang C. Current diagnostic and therapeutic strategies for COVID-19. Journal of Pharmaceutical Analysis. 2021;11(2):129-37.

[5] Zaim S, Chong JH, Sankaranarayanan V, Harky A. COVID-19 and multiorgan response. Current problems in cardiology. 2020;45(8):100618.

[6] Espinoza D, Rodriguez R, Kowalski A. 24 hours: a case of multiorgan failure associated with COVID-19. Cureus. 2020;12(8).

[7] Li N, Zhu L, Sun L, Shao G. The effects of novel coronavirus (SARS-CoV-2) infection on cardiovascular diseases and cardiopulmonary injuries. Stem Cell Research. 2021; 51:102168.

[8] Fernández-Quintela A, Milton-Laskibar I, Trepiana J, Gómez-Zorita S, Kajarabille N, Léniz A, González M, Portillo MP. Key aspects in nutritional management of COVID-19 patients. Journal of clinical medicine. 2020;9(8):2589.

[9] Singhal T. A review of coronavirus disease-2019 (COVID-19). The Indian journal of Pediatrics. 2020;87(4):281-286.

[10] Yang Y. Islam MS, Wang J, Li Y, Chen Traditional Chinese Medicine in the Treatment of Patients Infected with 2019-New Coronavirus (SARS-CoV-2): A Review and Perspective. International Journal of Biological Sciences.2020;16(10):1708-17.

[11] Park YL, Canaway R. Integrating traditional and complementary medicine with national healthcare systems for universal health coverage in Asia and the Western Pacific. Health Systems & Reform. 2019;5(1):24-31.

[12] Rudra S, Kalra A, Kumar A, Joe W. Utilization of alternative systems of medicine as health care services in India: Evidence on AYUSH care from NSS 2014. PloS one. 2017 ;12(5):0176916.

[13] Sen S, Chakraborty R. Revival, modernization and integration of Indian traditional herbal medicine in clinical practice: Importance, challenges and future. Journal of traditional and complementary medicine. 2017 ;7(2):234-44.

[14] Jain J, Pai S, Sunil S. Standardization of in vitro assays to evaluate the activity of polyherbal siddha formulations against Chikungunya virus infection. Virus disease. 2018; 29:32-9.

[15] Jain J, Kumar A, Narayanan V, Ramaswamy RS, Sathiyarajeswaran P, Devi MS, Kannan M, Sunil S. Antiviral activity of ethanolic extract of NilavembuKudineer against dengue and chikungunya virus through in vitro evaluation. Journal of Ayurveda and integrative medicine. 2020;11(3):329-35.

[16] Mahadevan H, Palraj V. Literature review on Siddha herbal formulations (Kudineer) available for the management of Dengue. International Journal of Pharmacology and Clinical Sciences. 2016;5(3).

[17] Prakash P, Meena R, Abraham LS, Sunkar S, Govindaraju K, Pully D, Samrot AV. Evidence-based traditional Siddha formulations for prophylaxis and management of respiratory symptoms in COVID-19 pandemic-a review. Biocatalysis and agricultural biotechnology. 2021 Aug 1; 35:102056.

[18] Kiran G, Karthik L, Devi MS, Sathiyarajeswaran P, Kanakavalli K, Kumar KM, Kumar DR. In silico computational screening of KabasuraKudineer-official Siddha formulation and JACOM against SARS-CoV-2 spike protein. Journal of Ayurveda and integrative medicine. 2022;13(1):100324.

[19] Saraswathi K, Arumugam P, Sivaraj C. Antioxidant evaluation and gas chromatography–mass spectrometry (GC–MS) profiling of aqueous dried tuberous roots of Asparagus racemosus Willd.: The queen of herbs. Journal of Pharmacognosy and Phytochemistry. 2020;9(3):466-76.

[20] O'Boyle NM, Banck M, James CA, Morley C, Vandermeersch T, Hutchison GR. Open Babel: An open chemical toolbox. Journal of cheminformatics. 2011;3(1):1-4.

[21] Fuhrmann J, Rurainski A, Lenhof HP, Neumann D. A new Lamarckian genetic algorithm for flexible ligand-receptor docking. Journal of computational chemistry. 2010;31(9):1911-8.

[22] Lipinski CA, Lombardo F, Dominy BW, Feeney PJ. Experimental and computational approaches to estimate solubility and permeability in drug discovery and development settings. Advanced drug delivery reviews.1997;23(1-3):3-25.

[23] Navia MA, Chaturvedi PR. Design principles for orally bioavailable

drugs. Drug discovery today. 1996;1(5):179-89

[24] Alex A, Millan DS, Perez M, Wakenhut F, Whitlock GA. Intramolecular hydrogen bonding to improve membrane permeability and absorption in beyond rule of five chemical space. MedChemComm. 2011;2(7):669-74.

[25] Benet LZ, Hosey CM, Ursu O, Oprea TI. BDDCS, the Rule of 5 and drugability. Advanced drug delivery reviews. 2016;101:89-98.

[26] Veber DF, Johnson SR, Cheng HY, Smith BR, Ward KW, Kopple KD. Molecular properties that influence the oral bioavailability of drug candidates. Journal of medicinal chemistry. 2002;45(12):2615-23.

[27] García-Godoy MJ, López-Camacho E, García-Nieto J, Nebro AJ, Aldana-Montes JF. Solving molecular docking problems with multi-objective metaheuristics. Molecules. 2015 ;20(6):10154-83.

[28] Kortemme T, Morozov AV, Baker D. An orientation-dependent hydrogen bonding potential improves prediction of specificity and structure for proteins and protein–protein complexes. Journal of molecular biology. 2003;326(4):1239-59.

[29] Zhang L, Lin D, Sun X, Curth U, Drosten C, Sauerhering L, Becker S, Rox K, Hilgenfeld R. Crystal structure of SARS-CoV-2 main protease provides a basis for design of improved α-ketoamide inhibitors. Science. 2020 ;368(6489):409-12.

[30] Mengist HM, Dilnessa T, Jin T. Structural basis of potential inhibitors targeting SARS-CoV-2 main protease. Frontiers in Chemistry. 2021;9:622898.

[31] Huang Y, Yang C, Xu XF, Xu W, Liu SW. Structural and functional properties of SARS-CoV-2 spike protein: potential antivirus drug development for COVID-19. Acta PharmacologicaSinica. 2020;41(9):1141-9.

[32] Papageorgiou AC, Mohsin I. The SARS-CoV-2 spike glycoprotein as a drug and vaccine target: structural insights into its complexes with ACE2 and antibodies. Cells. 2020;9(11):2343.

[33] Babcock GJ, Esshaki DJ, Thomas Jr WD, Ambrosino DM. Amino acids 270 to 510 of the severe acute respiratory syndrome coronavirus spike protein are required for interaction with receptor. Journal of virology. 2004 May 1;78(9):4552-60.

[34] Hoffmann M, Kleine-Weber H, Schroeder S, Krüger N, Herrler T, Erichsen S, Schiergens TS, Herrler G, Wu NH, Nitsche A, Müller MA. SARS-CoV-2 cell entry depends on ACE2 and TMPRSS2 and is blocked by a clinically proven protease inhibitor. cell. 2020;181(2):271-80.

[35] Keller C, Böttcher-Friebertshäuser E, Lohoff M. TMPRSS2, a novel host-directed drug target against SARS-CoV-2. Signal Transduction and Targeted Therapy. 2022;7(1):251.